Bayesian Detection for Distributed MIMO Radar with Non-Orthogonal Waveforms in Non-Homogeneous Clutter

Cengcang Zeng, Fangzhou Wang, and Hongbin Li
ECE Department, Stevens Institute of Technology
Hoboken, NJ 07030, USA

Mark A. Govoni
Army Research Laboratory
Adelphi, MD 20783, USA

***Abstract*—This paper considers target detection in distributed multi-input multi-output (MIMO) radar with non-orthogonal waveforms in non-homogenous clutter. We first present a general signal model for distributed MIMO radar in cluttered environments. To cope with the non-homogenous clutter and possible clutter bandwidth mismatch, the covariance matrix of the disturbance (clutter and noise) signal is modeled as a random matrix following an inverse complex Wishart distribution. Then, we propose three Bayesian detectors, including a non-coherent detector, a coherent detector, and a hybrid detector. The latter is a compromise of the former two, as it forsakes phase estimation needed by the coherent detector, but requires the samples within a coherent processing interval (CPI) to maintain phase coherence that is unnecessary for the non-coherent detector. Simulation results are presented to illustrate the performance of these Bayesian detectors and their non-Bayesian counterparts in non-homogeneous clutter when the clutter bandwidth is known exactly and, respectively, with uncertainty.**

***Index Terms*—Distributed MIMO radar, non-orthogonal waveforms, Bayesian detection, non-homogeneous clutter**

I. Introduction

In recent years, distributed multi-input multi-output (MIMO) radar, which employs widely separated antennas to form the transmit (TX) and receive (RX) apertures, has been of significant interest for civilian and military applications [1]–[5]. Compared with co-located MIMO radar, distributed MIMO radar can enhance target detection by exploiting the spatial diversity of the target's radar cross section (RCS) [6]. Target detection, a primary radar function, with distributed MIMO radar has received extensive attention [7]–[17]. A variety of detection techniques have been explored, such as adaptive detection [7], parametric clutter modeling [8], [9], utilization of a "defocused transmit-defocused" receive operating mode [10], power allocation [11], moving target detection on moving platforms [12], delay compensation [13], range-spread target detection [14], Bayesian detection in clutter [15], target residual due to imperfect waveform separation [16], and robust detection in the presence of clutter Doppler frequency mismatch [17].

While most prior studies assume orthogonal waveforms, orthogonality cannot be maintained across arbitrary propagation delays and Doppler frequency shifts [18]. To tackle this issue, target detection with general non-orthogonal waveforms in distributed MIMO radar was studied in [19], which also accounts for the effect of time, frequency, and phase errors among the transmitters and receivers. The work was recently extended to the case when the received signal contains non-negligible clutter [20].

In this paper, we continue investigating target detection for distributed MIMO radar with non-orthogonal waveforms in cluttered environments. While the clutter in distributed MIMO radar is inherently non-homogeneous with distinct power across different TX-RX pairs, the covariance matrix structure depends on the clutter bandwidth (BW), which is normally unknown. In practice, an upper bound for the clutter BW can be selected a priori to construct the covariance matrix, while the clutter power is adaptively estimated from the received signal [20]. However, a mismatch between the pre-selected upper bound and the exact clutter BW may exist, which could lead to performance degradation. To address this problem, we propose a Bayesian approach for target detection in non-homogeneous clutter by treating the disturbance (clutter plus noise) covariance matrix as a random matrix which follows an inverse complex Wishart distribution. Using this approach, we develop three Bayesian detectors using non-coherent, coherent, and hybrid detection. We compare the proposed Bayesian detectors with their non-Bayesian counterparts, which use a preselected clutter BW to construct the covariance matrix, in cases with and, respectively, without clutter BW mismatch.

II. Signal Model and Problem Formulation

Consider a distributed MIMO radar equipped with M widely separated TX antennas and N RX antennas. Each TX emits a succession of K pulses over a coherent processing interval (CPI). Suppose there is a moving target at distance $R_{\mathrm{t},m}$ to m-th TX and the distance $R_{\mathrm{r},n}$ to n-th RX. The range sum $R_{\mathrm{t},m}+R_{\mathrm{r},n}$ specifies an *isorange* of the (m,n)-th TX-RX pair with L_{mn} clutter scatterers, which is an ellipse with foci at the TX and RX. Then, the noise-free received signal at the RX can be expressed as [19]:

$$s_n(t)=\sum_{m=1}^{M}\alpha\xi_{mn}u_m(t-\tau_{mn})e^{\jmath\psi_{mn}}e^{\jmath 2\pi(f_{\mathrm{c}}+f_{mn})(t-\tau_{mn})}$$

This work was supported in part by the Army Research Office under Cooperative Agreement Number W911NF-19-2-0234 and the National Science Foundation under grants ECCS-1923739 and ECCS-2212940.

$$+\sum_{l=1}^{L_{mn}}\sum_{m=1}^{M}\widetilde{\alpha}_{mnl}\widetilde{\xi}_{mnl}u_m(t-\tau_{mn}) \times e^{\jmath\psi_{mn}}e^{\jmath 2\pi(f_c+\widetilde{f}_{mnl})(t-\tau_{mn})}, \quad (1)$$

where

- α and $\widetilde{\alpha}_{mnl}$ denote the radar cross section (RCS) of the target and, respectively, the (m,n,l)-th clutter scatterer.
- ξ_{mn} and $\widetilde{\xi}_{mnl}$ are the channel coefficients, which lump the path loss and antenna gains [19], associated with the (m,n)-th TX-RX pair of the target path and the (m,n,l)-th scatterer path, respectively.
- $u_m(t)=\sum_{k=0}^{K-1}p_m(t-kT_{\rm s})$ is the baseband transmitted signal which comprises K repetitions of the pulse waveform $p_m(t)$ with T_s being the pulse repetition interval.
- ψ_{mn} denotes the phase offset between the oscillators at the m-th TX and the n-th RX.
- $\tau_{mn}=(R_{{\rm t},m}+R_{{\rm r},n})/c$ is the propagation delay associated with the (m,n)-th TX-RX pair and c is the speed of light.
- f_c is the carrier frequency, while f_{mn} and $\widetilde{f}_{mnl}$ denote the Doppler frequency of the target and the (m,n,l)-th clutter scatterer.

After down conversion, the received signal passes through M matched filters (MFs) matched to the M radar waveforms and then is sampled at the radar pulse rate. The noise-free output sample of the m-th MF at the n-th RX corresponding to the k-th pulse, i.e., $x_{mn}(k)$, are stacked as a $K\times 1$ vector $\mathbf{x}_{mn}=[x_{mn}(0),\cdots,x_{mn}(K-1)]$:

$$\mathbf{x}_{mn}=\alpha\mathbf{S}_n\mathbf{h}_{mn}+\sum_{l}^{L_{mn}}\widetilde{\mathbf{S}}_{nl}\widetilde{\mathbf{h}}_{mnl}, \quad (2)$$

where

- $\mathbf{S}_n=[\mathbf{s}(f_{1n}),\cdots,\mathbf{s}(f_{Mn})]$ and $\widetilde{\mathbf{S}}_{nl}=[\mathbf{s}(\widetilde{f}_{1nl}),\cdots,\mathbf{s}(\widetilde{f}_{Mnl})]$ with $\mathbf{s}(f)=[1,e^{\jmath 2\pi T_{\rm s}f},\cdots,e^{\jmath 2\pi(K-1)T_{\rm s}f}]^T$.
- $\mathbf{h}_{mn}\in\mathbb{C}^{M\times 1}$ is the target channel vector with the $\bar{m}$-th element given by $[\mathbf{h}_{mn}]_{\bar{m}}=\xi_{\bar{m}n}e^{-\jmath 2\pi f_c\tau_{\bar{m}n}}e^{\jmath 2\pi f_{mn}(\tau_{mn}-\tau_{\bar{m}n})}e^{\jmath\psi_{mn}}\chi_{m\bar{m}}(\tau_{mn}-\tau_{\bar{m}n},f_{\bar{m}n}-f_{mn})$.
- $\widetilde{\mathbf{h}}_{mnl}\in\mathbb{C}^{M\times 1}$ is the clutter channel vector with the $\bar{m}$-th element given by $[\widetilde{\mathbf{h}}_{mnl}]_{\bar{m}}=\widetilde{\alpha}_{mnl}\widetilde{\xi}_{\bar{m}nl}e^{-\jmath 2\pi f_c\tau_{\bar{m}n}}e^{\jmath 2\pi f_{mn}(\tau_{mn}-\tau_{\bar{m}n})}e^{\jmath\psi_{mn}}\chi_{m\bar{m}}(\tau_{mn}-\tau_{\bar{m}n},f_{\bar{m}nl}-f_{mn})$.

The cross ambiguity function (CAF) $\chi_{m\bar{m}}(v,f)$ is defined as

$$\chi_{m\bar{m}}(\nu,f)=\int p_m(\mu)p^*_{\bar{m}}(\mu-\nu)e^{\jmath 2\pi f\mu}d\mu. \quad (3)$$

Since the clutter components contain reflections from unwanted stationary and slow moving objects (e.g., wind, rain, wave, etc.) within the considered test cell, their velocities and sizes are usually unknown. We assume that the clutter Doppler frequencies $\widetilde{f}_{\bar{m}nl}$ and reflection amplitudes $\alpha_{\bar{m}nl}$ are independent random variables. Specifically, $\widetilde{f}_{\bar{m}nl}$ are uniformly distributed in an interval of $[-\Delta_f,\Delta_f]$, where Δ_f denotes the maximum Doppler frequency, and $\widetilde{\alpha}_{\bar{m}nl}$ are Gaussian random variables with zero mean and variance $\sigma^2_{\bar{m}nl}$. Then, the (k_1,k_2)-th element of clutter covariance matrix $\mathbf{\Gamma}_{mn}$ can be expressed as

$$\begin{aligned}[\mathbf{\Gamma}_{mn}]_{k_1,k_2}&=\Big[\sum_{l}^{L_{mn}}\mathbb{E}\big[\widetilde{\mathbf{S}}_{nl}\widetilde{\mathbf{h}}_{mnl}\widetilde{\mathbf{h}}^H_{mnl}\widetilde{\mathbf{S}}^H_{nl}\big]\Big]_{k_1,k_2}\\ &\approx\Big[\sum_{l=1}^{L_{\bar{m}n}}\sum_{\bar{m}=1}^{M}|\widetilde{\chi}_{m\bar{m}n}|^2\mathbb{E}\big[\widetilde{\mathbf{S}}_{nl}\widetilde{\mathbf{\Lambda}}_{nl}\widetilde{\mathbf{S}}^H_{nl}\big]\Big]_{k_1,k_2}\\ &=\sum_{l=1}^{L_{\bar{m}n}}\sum_{\bar{m}=1}^{M}|\widetilde{\chi}_{m\bar{m}n}|^2\sigma^2_{\bar{m}nl}\widetilde{\xi}^2_{\bar{m}nl}{\rm sinc}[2\pi\Delta_f(k_1-k_2)T_{\rm s}]\\ &=a_{mn}[\mathbf{\Psi}]_{k_1,k_2}, \end{aligned} \quad (4)$$

where $\widetilde{\mathbf{\Lambda}}_{nl}$ is an $M\times M$ diagonal matrix with diagonal elements given by

$$[\widetilde{\mathbf{\Lambda}}_{nl}]_{\bar{m},\bar{m}}=\sigma^2_{\bar{m}nl}\widetilde{\xi}^2_{\bar{m}nl}, \quad (5)$$

and

$$a_{mn}=\sum_{l=1}^{L_{\bar{m}n}}\sum_{\bar{m}=1}^{M}|\widetilde{\chi}_{m\bar{m}n}|^2[\widetilde{\mathbf{\Lambda}}_{nl}]_{\bar{m},\bar{m}} \quad (6)$$

which denotes the clutter power with the approximation $\widetilde{\chi}_{m\bar{m}n}=\chi_{m\bar{m}}(\tau_{mn}-\tau_{\bar{m}n},0)\approx\chi_{m\bar{m}}(\tau_{mn}-\tau_{\bar{m}n},f_{\bar{m}nl}-f_{mn})$ as the radar waveform is insensitive to small Doppler shift [21, p.15], and

$$[\mathbf{\Psi}]_{k_1,k_2}={\rm sinc}[2\pi\Delta_f(k_1-k_2)T_{\rm s}],k_1,k_2=1,\cdots,K \quad (7)$$

which is the covariance structure matrix which depends on the clutter Doppler BW Δ_f with $T_{\rm s}$ being the pulse repetition interval.

Let $\mathbf{y}_{mn}$ denote the noise-contaminated observation of $\mathbf{x}_{mn}$. The moving target detection problem can be formulated as the following hypothesis testing:

$$\begin{aligned}\mathcal{H}_0&:\mathbf{y}_{mn}=\sum_{l}^{L_{mn}}\widetilde{\mathbf{S}}_{nl}\widetilde{\mathbf{h}}_{mnl}+\mathbf{w}_{mn},\\ \mathcal{H}_1&:\mathbf{y}_{mn}=\alpha\mathbf{S}_n\mathbf{h}_{mn}+\sum_{l}^{L_{mn}}\widetilde{\mathbf{S}}_{nl}\widetilde{\mathbf{h}}_{mnl}+\mathbf{w}_{mn},\\ &\qquad m=1,2,\cdots,M,\ n=1,2,\cdots,N,\end{aligned} \quad (8)$$

where $\mathbf{w}_{mn}$ is the noise with zero mean and covariance matrix $\sigma^2\mathbf{I}$, i.e., $\mathbf{w}_{mn}\sim\mathcal{CN}(\mathbf{0},\sigma^2\mathbf{I})$, and σ^2 is the noise variance.

Eqn. (4) indicates that the clutter has non-homogeneous power a_{mn}, which is distinct for different TX-RX pair, and its covariance matrix structure depends on the clutter BW Δ_f, which is generally unknown. A common approach is to choose an upper bound $\bar{\Delta}_f$ for Δ_f, while a_{mn} is estimated from the received signal [20]. If there is a mismatch between the upper bound and the real clutter BW, a performance loss is expected. To address this problem, we consider a Bayesian approach as described next.

Let $\mathbf{d}_{mn}$ denote the disturbance signal that includes the

clutter and noise:

$$\mathbf{d}_{mn} = \sum_{l}^{L_{mn}} \widetilde{\mathbf{S}}_{nl} \widetilde{\mathbf{h}}_{mnl} + \mathbf{w}_{mn}, \tag{9}$$

whose covariance matrix is denoted by $\mathbf{R}_{mn}$. We have $\mathbf{R}_{mn} = a_{mn}\mathbf{\Psi} + \sigma^2\mathbf{I} \approx a_{mn}(\mathbf{\Psi} + \sigma^2\mathbf{I})$ because the clutter is usually much stronger than the noise. To account for the non-homogeneous clutter power and possible clutter BW mismatch, we model $\mathbf{R}_{mn}$ as a complex inverse Wishart random matrix [14]:

$$\mathbf{R}_{mn} \backsim \mathcal{CW}^{-1}\big(a_{mn}(v-K)\widetilde{\mathbf{\Psi}}, v\big), \tag{10}$$

where v is the degree of freedom of the inverse Wishart distribution and $(v-K)\widetilde{\mathbf{\Psi}}$ denotes a prior knowledge of the covariance matrix with $\widetilde{\mathbf{\Psi}} = \mathbf{\Psi} + \sigma^2\mathbf{I}$. The probability density function (PDF) of $\mathbf{R}_{mn}$ conditioned on a_{mn} is given by

$$f(\mathbf{R}_{mn}|a_{mn}) = \frac{|a_{mn}(v-K)\widetilde{\mathbf{\Psi}}|^v}{\bar{\Gamma}_K(v)|\mathbf{R}_{mn}|^{(v+K)}} e^{\mathrm{tr}(-(v-K)a_{mn}\widetilde{\mathbf{\Psi}}\mathbf{R}_{mn}^{-1})}, \tag{11}$$

where

$$\bar{\Gamma}_K(v) = \pi^{\frac{K(K-1)}{2}} \prod_{k=1}^{K} \Gamma(v-k+1) \tag{12}$$

denotes the multivariate gamma function which can be defined in terms of the original gamma function $\Gamma(\cdot)$. In the next section, we develop three Bayesian detectors based on this model, referred to as Bayesian non-coherent detector in clutter (B-NCDC), Bayesian coherent detector in clutter (B-CDC), and Bayesian hybrid detector in clutter (B-HDC), respectively.

III. Bayesian Detectors in Clutter

A. B-NCDC

The B-NCDC treats the target signal in (8) as an unknown quantity with no specific structure, i.e., $\boldsymbol{\mu}_{mn} = \alpha\mathbf{S}_n\mathbf{h}_{mn}$, and solves the detection problem using a generalized likelihood ratio test (GLRT) approach along with the maximum likelihood estimates (MLEs) of the unknown parameters. Specifically, the GLRT is given by the likelihood ratio with the parameters replaced by their MLEs:

$$\frac{\max\limits_{\{\boldsymbol{\mu}_{mn}\},\{\mathbf{R}_{mn}\}} \prod\limits_{m,n} \int f_1(\mathbf{y}_{mn}|\boldsymbol{\mu}_{mn},\mathbf{R}_{mn}) f(\mathbf{R}_{mn}|a_{mn}) d\mathbf{R}_{mn}}{\max\limits_{\{\mathbf{R}_{mn}\}} \prod\limits_{m,n} \int f_0(\mathbf{y}_{mn}|\mathbf{R}_{mn}) f(\mathbf{R}_{mn}|a_{mn}) d\mathbf{R}_{mn}} \tag{13}$$

where

$$f_1(\mathbf{y}_{mn}|\boldsymbol{\mu}_{mn},\mathbf{R}_{mn}) = \frac{\exp\Big(-\mathrm{tr}\big((\mathbf{R}_{mn})^{-1}\widetilde{\mathbf{y}}_{mn}\widetilde{\mathbf{y}}_{mn}^H\big)\Big)}{\pi^K \det(\mathbf{R}_{mn})} \tag{14}$$

$$f_0(\mathbf{y}_{mn}|\mathbf{R}_{mn}) = \frac{\exp\Big(-\mathrm{tr}\big((\mathbf{R}_{mn})^{-1}\mathbf{y}_{mn}\mathbf{y}_{mn}^H\big)\Big)}{\pi^K \det(\mathbf{R}_{mn})}, \tag{15}$$

and $\widetilde{\mathbf{y}}_{mn} = \mathbf{y}_{mn} - \boldsymbol{\mu}_{mn}$. Substituting (11), (14), and (15) into (13) followed by simplification yields

$$\prod_{m,n} \frac{\max\limits_{\boldsymbol{\mu}_{mn},a_{mn}} a_{mn}^K |\widetilde{\mathbf{y}}_{mn}\widetilde{\mathbf{y}}_{mn}^H + a_{mn}(v-K)\widetilde{\mathbf{\Psi}}|^{-(v+1)}}{\max\limits_{a_{mn}} a_{mn}^K |\mathbf{y}_{mn}\mathbf{y}_{mn}^H + a_{mn}(v-K)\widetilde{\mathbf{\Psi}}|^{-(v+1)}}. \tag{16}$$

The MLE of a_{mn} under $\mathcal{H}_1$ is obtained by

$$\begin{aligned}&\max_{a_{mn}} a_{mn}^{Kv} |\widetilde{\mathbf{y}}_{mn}\widetilde{\mathbf{y}}_{mn}^H + a_{mn}(v-K)\widetilde{\mathbf{\Psi}}|^{-(v+1)} \\ =&\min_{a_{mn}} a_{mn}^{\frac{K}{v+1}} (1 + a_{mn}^{-1}\widetilde{\mathbf{y}}_{mn}((v-K)\widetilde{\mathbf{\Psi}})^{-1}\widetilde{\mathbf{y}}_{mn}^H).\end{aligned} \tag{17}$$

Taking the derivative of the log of the above equation with respect to a_{mn} and setting it to zero, we obtain the MLE of a_{mn} under $\mathcal{H}_1$ as:

$$\hat{a}_{mn,1} = \frac{v+1-K}{K} \widetilde{\mathbf{y}}_{mn}^H ((v-K)\widetilde{\mathbf{\Psi}})^{-1} \widetilde{\mathbf{y}}_{mn}. \tag{18}$$

Substituting the above MLE of a_{mn} into the numerator of (16), the MLE of μ_{mn} under $\mathcal{H}_1$ is given by

$$\hat{\boldsymbol{\mu}}_{mn} = \mathbf{y}_{mn}.$$

Similarly, the MLE of a_{mn} under $\mathcal{H}_0$ can be shown to be

$$\hat{a}_{mn,0} = \frac{v+1-K}{K} \mathbf{y}_{mn}^H ((v-K)\widetilde{\mathbf{\Psi}})^{-1} \mathbf{y}_{mn}. \tag{19}$$

Substituting the MLEs under $\mathcal{H}_1$ and $\mathcal{H}_0$, i.e., $\hat{a}_{mn,1}$, $\hat{\boldsymbol{\mu}}_{mn}$ and $\hat{a}_{mn,0}$, into (16), the B-NCDC reduces to:

$$\begin{aligned}T_{\text{B-NCDC}} = &\prod_{m,n} \big(\mathbf{y}_{mn}^H \widetilde{\mathbf{\Psi}}^{-1} \mathbf{y}_{mn} \\ &\times |\mathbf{y}_{mn}\mathbf{y}_{mn}^H + \frac{v+1-K}{K} \mathbf{y}_{mn}^H \widetilde{\mathbf{\Psi}}^{-1} \mathbf{y}_{mn} \widetilde{\mathbf{\Psi}}|\big) \\ &\underset{\mathcal{H}_0}{\overset{\mathcal{H}_1}{\gtrless}} \gamma_{\text{B-NCDC}}.\end{aligned} \tag{20}$$

B. B-CDC

Next, we propose a coherent detector under the condition that the carrier phase can be accurately tracked and exploited for compensation, which enables improved detection performance. Specifically, the receiver forms the target Doppler matrix $\mathbf{S}_n$ and channel vector $\mathbf{h}_{mn}$. This leaves the target RCS α as the only unknown target parameter under $\mathcal{H}_1$. Then, the B-CDC can be obtained by using the GLRT framework as:

$$\frac{\max\limits_{\alpha,\{a_{mn}\}} \prod\limits_{m,n} \int f_1(\mathbf{y}_{mn}|\alpha,\mathbf{R}_{mn}) f(\mathbf{R}_{mn}|a_{mn}) d\mathbf{R}_{mn}}{\max\limits_{\{a_{mn}\}} \prod\limits_{m,n} f_0(\mathbf{y}_{mn}|\mathbf{R}_{mn}) f(\mathbf{R}_{mn}|a_{mn}) d\mathbf{R}_{mn}}, \tag{21}$$

where the likelihood function under $\mathcal{H}_1$ is similar to (13) for B-NCDC except that the mean $\boldsymbol{\mu}_{mn}$ is replaced by its structured version $\alpha\mathbf{S}_n\mathbf{h}_{mn}$, while the likelihood function under $\mathcal{H}_0$ is the same as in (13). Thus, the MLE of a_{mn} under $\mathcal{H}_0$ is given by (19). The MLEs of α and a_{mn} under $\mathcal{H}_1$ can be similarly obtained in a sequential manner as for the B-NCDC:

$$\hat{a}_{mn,1} = \frac{v+1-K}{K} \widetilde{\mathbf{y}}_{mn}^H \big((v-K)\widetilde{\mathbf{\Psi}}\big)^{-1} \widetilde{\mathbf{y}}_{mn}. \tag{22}$$

and

$$\hat{\alpha} = \frac{\mathbf{h}_{mn}^H \mathbf{S}_n^H \widetilde{\boldsymbol{\alpha}}^{-1} \mathbf{y}_{mn}}{\mathbf{h}_{mn}^H \mathbf{S}_n^H \widetilde{\boldsymbol{\alpha}}^{-1} \mathbf{S}_n \mathbf{h}_{mn}}. \tag{23}$$

Then, substituting the MLEs back into (21), the B-CDC is given by

$$T_{\text{B-CDC}} = \prod_{m,n} \frac{|\mathbf{y}_{mn}\mathbf{y}_{mn}^H + \frac{v+1-K}{K}\mathbf{y}_{mn}^H \widetilde{\boldsymbol{\Psi}}^{-1}\mathbf{y}_{mn}\widetilde{\boldsymbol{\Psi}}|}{|\widetilde{\mathbf{y}}_{mn}\widetilde{\mathbf{y}}_{mn}^H + \frac{v+1-K}{K}\widetilde{\mathbf{y}}_{mn}^H \widetilde{\boldsymbol{\Psi}}^{-1}\widetilde{\mathbf{y}}_{mn}\widetilde{\boldsymbol{\Psi}}|} \times \frac{(\mathbf{h}_{mn}^H \mathbf{S}_n^H \widetilde{\boldsymbol{\Psi}}^{-1}\mathbf{S}_n \mathbf{h}_{mn})(\mathbf{y}_{mn}^H \widetilde{\boldsymbol{\Psi}}^{-1}\mathbf{y}_{mn})}{(\mathbf{h}_{mn}^H \mathbf{S}_n^H \widetilde{\boldsymbol{\Psi}}^{-1}\mathbf{S}_n \mathbf{h}_{mn})(\mathbf{y}_{mn}^H \widetilde{\boldsymbol{\Psi}}^{-1}\mathbf{y}_{mn}) - |\mathbf{h}_{mn}^H \mathbf{S}_n^H \widetilde{\boldsymbol{\Psi}}^{-1}\mathbf{y}_{mn}|^2} \underset{\mathcal{H}_0}{\overset{\mathcal{H}_1}{\gtrless}} \gamma_{\text{B-CDC}}. \tag{24}$$

C. B-HDC

As noted earlier, B-HDC is a comprise between the B-NCDC and B-CDC. Specifically, let $\boldsymbol{\beta}_{mn} = \alpha \mathbf{h}_{mn}$. The B-HDC can be obtained by using GLRT as

$$\frac{\max\limits_{\{\boldsymbol{\beta}_{mn}\},\{a_{mn}\}} \prod\limits_{m,n} \int f_1(\mathbf{y}_{mn}|\boldsymbol{\beta}_{mn}, \mathbf{R}_{mn}) f(\mathbf{R}_{mn}|a_{mn}) d\mathbf{R}_{mn}}{\max\limits_{\{a_{mn}\}} \prod\limits_{m,n} f_0(\mathbf{y}_{mn}|\mathbf{R}_{mn}) f(\mathbf{R}_{mn}|a_{mn}) d\mathbf{R}_{mn}}. \tag{25}$$

Since the MLE of a_{mn} under $\mathcal{H}_0$ is given by (13), we only need to solve the estimation problem under $\mathcal{H}_1$. Following a similar sequential procedure used for the B-NCDC by setting the mean vector $\boldsymbol{\mu}_{mn} = \mathbf{S}_n \boldsymbol{\beta}_{mn}$, we can obtain the MLEs under $\mathcal{H}_1$ as

$$\hat{a}_{mn,1} = \frac{v+1-K}{K} \widetilde{\mathbf{y}}_{mn}^H ((v-K)\widetilde{\boldsymbol{\Psi}})^{-1} \widetilde{\mathbf{y}}_{mn}, \tag{26}$$

and

$$\hat{\boldsymbol{\beta}}_{mn} = \frac{\mathbf{S}_n^H \widetilde{\boldsymbol{\Psi}}^{-1} \mathbf{y}_{mn}}{\mathbf{S}_n^H \widetilde{\boldsymbol{\Psi}}^{-1} \mathbf{S}_n}. \tag{27}$$

Finally, the Bayesian-based hybrid detector in clutter (B-HDC) can be expressed as

$$T_{\text{B-HDC}} = \prod_{m,n} \frac{|\mathbf{y}_{mn}\mathbf{y}_{mn}^H + \frac{v+1-K}{K}\mathbf{y}_{mn}^H \widetilde{\boldsymbol{\Psi}}^{-1}\mathbf{y}_{mn}\widetilde{\boldsymbol{\Psi}}|}{|\widetilde{\mathbf{y}}_{mn}\widetilde{\mathbf{y}}_{mn}^H + \frac{v+1-K}{K}\widetilde{\mathbf{y}}_{mn}^H \widetilde{\boldsymbol{\Psi}}^{-1}\widetilde{\mathbf{y}}_{mn}\widetilde{\boldsymbol{\Psi}}|} \times \frac{(\mathbf{S}_n^H \widetilde{\boldsymbol{\Psi}}^{-1}\mathbf{S}_n)(\mathbf{y}_{mn}^H \widetilde{\boldsymbol{\Psi}}^{-1}\mathbf{y}_{mn})}{(\mathbf{S}_n^H \widetilde{\boldsymbol{\Psi}}^{-1}\mathbf{S}_n)(\mathbf{y}_{mn}^H \widetilde{\boldsymbol{\Psi}}^{-1}\mathbf{y}_{mn}) - |\mathbf{S}_n^H \widetilde{\boldsymbol{\Psi}}^{-1}\mathbf{y}_{mn}|^2} \underset{\mathcal{H}_0}{\overset{\mathcal{H}_1}{\gtrless}} \gamma_{\text{B-HDC}}. \tag{28}$$

IV. Simulation Results

In this section, simulation results are presented to show the performance of the B-NCDC, B-CDC, and B-HDC and their non-Bayesian counterparts NCDC, CDC, and HDC introduced in [20]. In addition, we also include for comparison the NCD, CD, and HD detectors in [19], which were introduced for target detection in the absence of clutter (noise only). Two scenarios are considered. The first one is an ideal case where there is no mismatch between the prior knowledge, which refers to the clutter Doppler BW, and the ground truth, whereas the other one involves a mismatch.

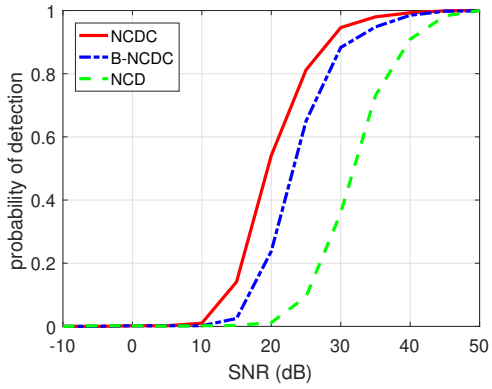

(a)

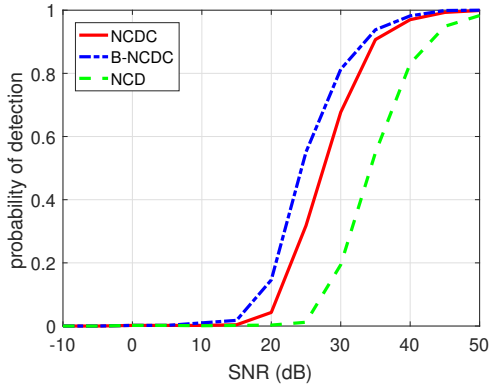

(b)

Figure 1. Probability of detection versus SNR for non-coherent detectors when CNR = 30 dB: (a) Without model mismatch; (b) With model mismatch.

In the simulation, a distributed MIMO radar with $M = 2$ TXs and $N = 1$ RX is considered. The propagation delays are $\tau_{11} = 0.1T_p$ and $\tau_{21} = 0.61T_p$, where $T_p = 10^{-5}$ s is the pulse duration. The pulse repetition frequency (PRF) is 500 Hz, the carrier frequency is 3 GHz, and the normalized target Doppler frequencies are $f_{11} = 0.3$ and $f_{21} = 0.4$. From (4), we set the prior knowledge of the clutter Doppler BW to $\bar{\Delta}_f = 0.12$ and denote by Δ_f the real Doppler BW.

The signal-to-noise ratio (SNR) and clutter-to-noise ratio (CNR) are defined as

$$\text{SNR} = \sum_{m=1}^{M} \sum_{n=1}^{N} \frac{|\xi_{mn}|^2 \mathbb{E}\{|\alpha|^2\}}{\sigma^2}, \tag{29}$$

and

$$\text{CNR} = \sum_{m=1}^{M} \sum_{n=1}^{N} \sum_{l=1}^{L_{mn}} \frac{|\xi_{mnl}|^2 \mathbb{E}\{|\widetilde{\alpha}_{mnl}|^2\}}{\sigma^2}. \tag{30}$$

where σ^2 is the noise variance. In addition, the target RCS and clutter RCS are randomly generated with complex Gaussian distribution, i.e., $\alpha \sim \mathcal{CN}(0, \sigma_{\text{t}}^2)$ and $\widetilde{\alpha}_{mnl} \sim \mathcal{CN}(0, \sigma_{mnl}^2)$, where σ_{t}^2 and σ_{mnl}^2 are determined based on specific values of

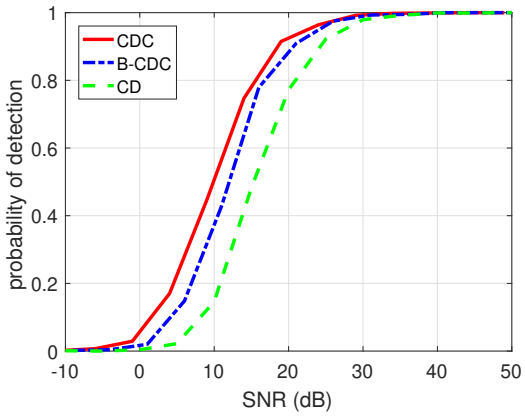

(a)

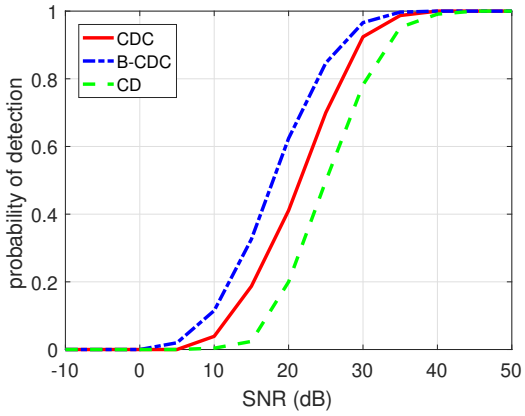

(b)

Figure 2. Probability of detection versus SNR for coherent detectors when CNR = 30 dB: (a) Without model mismatch; (b) With model mismatch.

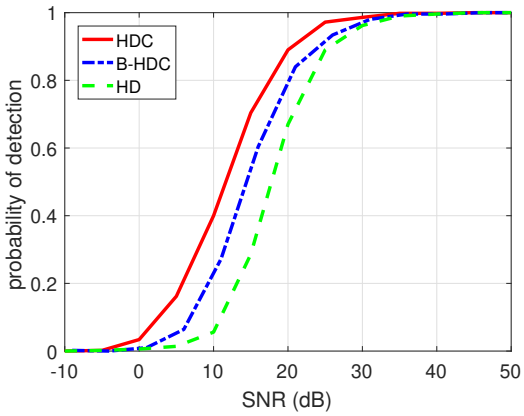

(a)

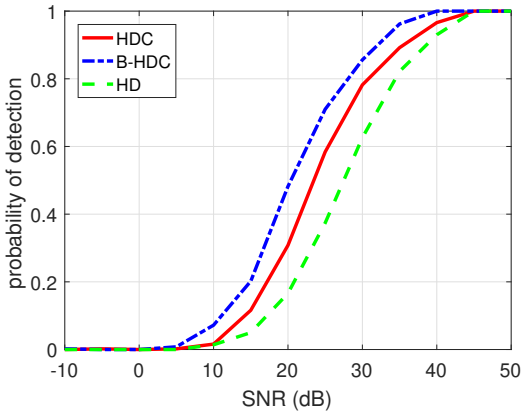

(b)

Figure 3. Probability of detection versus SNR for hybrid detectors when CNR = 30 dB: (a) Without model mismatch; (b) With model mismatch.

SNR and CNR, respectively. Other simulation parameters are set as follows: the number of pulses within a CPI is $K = 10$ and the probability of false alarm is $P_f = 10^{-4}$.

Fig. 1(a) shows the performance of NCDC, N-NCDC and NCD when $\Delta_f = \bar{\Delta}_f = 0.12$, i.e., there is no mismatch between the prior knowledge and real knowledge. It can be observed that the performance of NCDC is better than B-NCDC because the Bayesian approach imposes an additional model and involves a more complex estimation process. However, when there is a mismatch between the prior knowledge and real knowledge, as shown in Fig. 1(b) with $\Delta_f = 0.24$ and $\bar{\Delta}_f = 0.12$, B-NCDC has the best detection performance because the Bayesian-based detector can partially correct the prior knowledge error by using Bayesian estimation, which utilizes not only the prior knowledge, but also the measured data for estimation. In this sense, B-NCDC is a robust solution that is able to tolerate some model mismatch, at the price of slight performance loss when there is no model mismatch. Note that in Fig. 1(b), all detectors experience some degradation compared with Fig. 1(a). This is because with $\Delta_f = 0.24$, the clutter has a larger BW (doubled) and is closer to the targets, which makes target detection harder due to stronger clutter leakage, i.e., more clutter power being leaked into the target band.

Similar relations can be observed in Figs. 2 and 3 for the coherent detectors and hybrid detectors. In addition, by comparing these figures, it can be seen that the detection performance of B-CDC is better than that of B-NCDC, while B-HDC is between the two but is much closer to B-CDC. This makes B-HDC a good choice in cases when accurate phase estimation is infeasible, which precludes B-CDC. As explained earlier, B-HDC requires the signal samples within a CPI to maintain phase coherence, which is generally ensured in Doppler processing based radar systems by design. In contrast, the non-coherent B-NCDC does not exploit this property for detection, which incurs a significant performance loss.

V. Conclusions

In this paper, a new Bayesian approach is introduced for target detection in distributed MIMO radar with non-orthogonal waveforms and non-homogenous clutter. To tackle non-homogenous clutter power and possible mismatch of the clutter Doppler BW, we proposed a stochastic model for the disturbance (clutter plus noise) covariance matrix. Based on this model, we developed three Bayesian detectors including

the B-NCDC, B-CDC, and B-HDC. Comparison between the proposed Bayesian detectors and their non-Bayesian counterparts were made. Simulation results indicate that the Bayesian detectors are robust against clutter BW mismatch.

REFERENCES

[1] A. M. Haimovich, R. S. Blum, and L. J. Cimini, "MIMO radar with widely separated antennas," *IEEE Signal Processing Magazine*, vol. 25, no. 1, pp. 116–129, 2008.

[2] P. Wang, H. Li, and B. Himed, "Moving target detection using distributed MIMO radar in clutter with nonhomogeneous power," *IEEE Transactions on Signal Processing*, vol. 59, no. 10, pp. 4809–4820, 2011.

[3] Q. He, R. S. Blum, H. Godrich, and A. M. Haimovich, "Target velocity estimation and antenna placement for MIMO radar with widely separated antennas," *IEEE Journal of Selected Topics in Signal Processing*, vol. 4, no. 1, pp. 79–100, 2010.

[4] C. Zeng, F. Wang, H. Li, and M. A. Govoni, "New coherent and hybrid detectors for distributed MIMO radar with synchronization errors," in *2021 IEEE Radar Conference (RadarConf21)*, 2021, pp. 1–5.

[5] H. Li, Z. Wang, J. Liu, and B. Himed, "Moving target detection in distributed MIMO radar on moving platforms," *IEEE Journal of Selected Topics in Signal Processing*, vol. 9, no. 8, pp. 1524–1535, 2015.

[6] E. Fishler, A. Haimovich, R. S. Blum, L. J. Cimini, D. Chizhik, and R. A. Valenzuela, "Spatial diversity in radarsmodels and detection performance," *IEEE Transactions on signal processing*, vol. 54, no. 3, pp. 823–838, 2006.

[7] Q. Hu, H. Su, S. Zhou, Z. Liu, and J. Liu, "Target detection in distributed MIMO radar with registration errors," *IEEE Transactions on Aerospace and Electronic Systems*, vol. 52, no. 1, pp. 438–450, 2016.

[8] P. Wang, H. Li, and B. Himed, "A parametric moving target detector for distributed MIMO radar in non-homogeneous environment," *IEEE Transactions on Signal Processing*, vol. 61, no. 9, pp. 2282–2294, 2013.

[9] L. Zhu, G. Wen, Y. Liang, D. Luo, and H. Song, "Parametric wald test for target detection with distributed MIMO radar in partially mixing homogeneous and non-homogeneous environments," *IET Radar, Sonar & Navigation*, vol. 16, no. 3, pp. 470–486, 2022.

[10] S. Yang, W. Yi, and A. Jakobsson, "Multi-target detection strategy for distributed MIMO radar with widely separated antennas," *IEEE Transactions on Geoscience and Remote Sensing*, 2022.

[11] S. Jebali, H. Keshavarz, and M. Allahdadi, "Joint power allocation and target detection in distributed MIMO radars," *IET Radar, Sonar & Navigation*, vol. 15, no. 11, pp. 1433–1447, 2021.

[12] P. Chen, L. Zheng, X. Wang, H. Li, and L. Wu, "Moving target detection using colocated MIMO radar on multiple distributed moving platforms," *IEEE Transactions on Signal Processing*, vol. 65, no. 17, pp. 4670–4683, 2017.

[13] C. Zeng, F. Wang, H. Li, and M. A. Govoni, "Delay compensation for distributed MIMO radar with non-orthogonal waveforms," *IEEE Signal Processing Letters*, vol. 29, pp. 41–45, 2021.

[14] Y. Gao, H. Li, and B. Himed, "Knowledge-aided range-spread target detection for distributed MIMO radar in nonhomogeneous environments," *IEEE Transactions on Signal Processing*, vol. 65, no. 3, pp. 617–627, 2016.

[15] J. Liu, J. Han, Z.-J. Zhang, and J. Li, "Bayesian detection for MIMO radar in gaussian clutter," *IEEE Transactions on Signal Processing*, vol. 66, no. 24, pp. 6549–6559, 2018.

[16] P. Wang and H. Li, "Target detection with imperfect waveform separation in distributed MIMO radar," *IEEE Transactions on Signal Processing*, vol. 68, pp. 793–807, 2020.

[17] A. Hassanien, B. Himed, and B. D. Rigling, "Robust moving target detection for distributed MIMO radar in non-homogeneous clutter," in *2019 International Radar Conference (RADAR)*. IEEE, 2019, pp. 1–6.

[18] Y. I. Abramovich and G. J. Frazer, "Bounds on the volume and height distributions for the MIMO radar ambiguity function," *IEEE Signal Processing Letters*, vol. 15, pp. 505–508, 2008.

[19] H. Li, F. Wang, C. Zeng, and M. A. Govoni, "Signal detection in distributed MIMO radar with non-orthogonal waveforms and sync errors," *IEEE Transactions on Signal Processing*, vol. 69, pp. 3671–3684, 2021.

[20] C. Zeng, F. Wang, H. Li, and M. A. Govoni, "Target detection for distributed MIMO radar with non-orthogonal waveforms in cluttered environments," *[Manuscript submitted for publication]*, 2022.

[21] J. Ward, "Space-time adaptive processing for airborne radar," Massachusetts Inst of Tech Lexington Lincoln Lab, Tech. Rep., 1994.